Proceedings World Geothermal Congress 2000
Kyushu - Tohoku, Japan, May 28 - June 10, 2000

GROWTH PROCESS OF THE RESERVOIR IN THE YUNOMORI HDR/HWR TEST SITE --- AN APPROACH BASED ON A MODEL OF RESERVOIR GROWTH IN THE SHEAR MODE ---

Kazuo HAYASHI and Keiichi MINAMIURA
Institute of Fluid Science, Tohoku University, Sendai 980-8577, Japan

Key words: HDR, HWR, reservoir crack, hydraulic stimulation, hydraulic fracturing

ABSTRACT

HDR/HWR reservoirs consist of multiple cracks which are either natural or artificial. In this paper, we examine the growth process and change in morphology of such reservoirs during hydraulic stimulation. To this end, we first construct a model based on shear dilation due to self-propping induced by frictional shear slip along preexisting planes of weakness. Then, we apply the model to the reservoir created by hydraulic stimulation performed through well TG-2 at the Yunomori test site of the HWR project of the New Energy and Industrial Development Organization (NEDO), Japan. In the application, we employ the data estimated by spinner logging and FMI (Formation Micro Imager) survey. Through spinner logging, four zones of well TG-2 have been identified to accept the injected fluid. The orientation of the cracks in each of the four zones has been identified through the FMI survey. Roughly speaking, two sets of cracks are predominant in the test site, i.e., almost horizontal cracks and almost vertical cracks which are striking in the northwest direction. We also employed the stress field estimated by the ASR (anelastic strain recovery) method. It is revealed that the morphology and growth process of the reservoir at the test site is dependent on the injection flow rate during the hydraulic stimulation. For a small injection flow rate, the vertical cracks of all the four zones and horizontal cracks in the shallower two zones are active. For a large injection flow rate, all cracks of the four zones become active to accept the injected fluid. Regarding the contribution of the four zones to accept the injected fluid, the shallower two zones play a major role for a small injection rate. For example, all the injected fluid flows into the shallower two zones for the injection flow rate that is less than $50\,m^3/h$. However, for the injection flow rate of $500\,m^3/h$, 30% of the injected fluid flows into the shallower two zones while the remaining 70% flows into the deeper two zones. The transition takes place at around the injection flow rate of 200-300 m^3/h. The morphology of the reservoir estimated by the present model fairly well agrees with the estimation obtained by using the location of AE (acoustic emission) events observed during the hydraulic stimulation.

1. INTRODUCTION

Engineered/stimulated reservoirs are used in HDR (Hot Dry Rock) and HWR (Hot Wet Rock) geothermal heat extraction (Duchane, 1991; Takahashi and Hashida, 1992). During the last decade, a variety of models of a reservoir consisting of a crack network have been proposed. An excellent review of these models has been provided by Willis-Richards and Wallroth(1995). Qualitatively, an ellipsoidal reservoir is supposed to be created by hydraulic stimulation in a rock mass with a natural crack network. The direction of the major axis of the ellipsoidal reservoir is approximately parallel to the maximum compressive stress direction. In all of the models, the Darcy's law has been employed for expressing the fluid flow within the reservoir cracks. However, during hydraulic stimulation fluid is injected at a flow rate of more than $200\,m^3/h$ into a formation through a finite number of thin cracks with aperture of several millimeters. Moreover, there is a tendency in some cases for the bottom hole pressure to continue to increase with time even if injection flow rate is kept constant. These imply that fluid flow would be turbulent in the cracks that are at least near the wellbore. Furthermore, there are experimental evidences that HDR reservoirs created by hydraulic stimulation do not necessarily have innumerable flow paths but several main flow paths, e.g. five main paths in the Hijiori field (Miyairi, 1993) and eight main paths in the Fenton Hill field (Fehler et al., 1987). Under these considerations, Hayashi and Taniguchi (1999) introduced a simple model that feature turbulent flow in cracks growing along pre-existing planes of weakness, where the deformation mode of the cracks was supposed to be a pure opening mode. We applied the model to a set of field data obtained during a hydraulic stimulation.

The pure opening mode is one of the ideal extreme situations of crack deformation. The other ideal extreme situation is pure shear mode. What happens in the field is between the two extreme situations, depending primarily on the stress orientation and orientation of pre-existing planes of weakness. Based on the concept that the increase in the aperture of geothermal reservoir cracks is primarily due to self-propping formed by slip induced along pre-existing planes of weakness, we construct in this paper a simple model that can describe the transitional morphology of geothermal reservoirs due to injection flow rate during hydraulic stimulation. We apply the model to examine and to understand what happened during hydraulic stimulation performed at well TG-2 in the Yunomori test site of the HWR project of NEDO.

2. MODEL OF THE RESERVOIR FORMED BY SLIP ALONG PLANES OF WEAKNESS

Let us consider a crack along a plane of weakness (Figure 1). The crack is connected to a wellbore and the injected fluid flows into the crack. Let us assume the fluid flow in the crack is radial and turbulent. We adopt the following equation for a first order approximation from Jung (1986):

$$\frac{dp}{dr} = -\frac{\lambda}{8w^3} 2\rho q^2 \qquad (1)$$

$$q = vw \qquad (2)$$

where p is the pressure of the fluid in the crack, r is the radial distance from the center of the wellbore, w is the aperture of the crack, ρ is the density of fluid, q is the flow rate measured per unit length in the circumferential direction and v is the velocity of the radial flow. The velocity v is given by $Q/(2\pi wr)$ where Q is the flow rate flowing into the crack from the well-bore. The coefficient λ represents the fluid flow resistance defined as follows (Jung, 1986):

$$\lambda = \frac{0.15}{[\log\{(k/D_h)/1.24\}]^2} \tag{3}$$

where k is the roughness of the crack surface and D_h (= 2 w) is the hydraulic diameter of the flow path along the crack.

The pressure distribution in the crack is given by

$$p = p_0 + \int_0^r \left\{ -\frac{\lambda}{8w^3} 2\rho \left(\frac{Q}{2\pi r} \right) \right\} dr$$

$$= p_0 - \alpha \left(1 - \frac{r_0}{r} \right) \tag{4}$$

where p_0 is the bottom hole pressure, a is the crack size and α defined as follows, is a measure of the pressure decrease along the crack:

$$\alpha = \frac{\lambda}{8w^3} 2\rho \left(\frac{Q}{2\pi} \right)^2 \frac{1}{r_0} \tag{5}$$

The average $\bar{p}$ of the pressure within the crack is given by

$$\bar{p} = \frac{1}{\pi(a^2 - r_0^2)} \int_0^{2\pi} d\theta \int_0^a \left\{ p_0 - \frac{\lambda}{8w^3} 2\rho \left(\frac{Q}{2\pi} \right) \frac{1}{r_0} \left(1 - \frac{r_0}{r} \right) \right\} dr$$

$$= p_0 - \alpha \left(1 - 2\frac{r_0}{a} \right) \tag{6}$$

Let us suppose that the following equation is applicable on the crack induced by slip along a plane of weakness:

$$\tau - (\sigma - p)\tan(\phi + i) = 0 \tag{7}$$

where σ is the normal stress acting perpendicularly to the crack, τ the shear stress along the crack surface, ϕ the angle of friction and i the shear dilation angle (Willis-Richards et al., 1996). In eq. (7), let us use the average of the fluid pressure in the crack, $\bar{p}$ instead of the local value of the fluid pressure in the crack, p .'We then obtain

$$p_0 = \sigma - \frac{\tau}{\tan(\phi + i)} + \alpha \left(1 - 2\frac{r_0}{a} \right) \tag{8}$$

Now, let us construct a simple model of hydraulic stimulation for a rock mass with many planes of weakness. Let N be the total number of the planes of weakness that becomes active to accept the fluid by the hydraulic stimulation. We then have the following expression for each activated crack:

$$p_{on} = S_n + f_n Q_n^2 \qquad (n = 1,2,\cdots,N) \tag{9}$$

where Q_n is the flow rate of fluid flowing into the n -th crack and

$$S_n = \sigma_n - \frac{\tau_n}{\tan(\phi + i)} \tag{10}$$

$$f_n = \frac{\lambda}{8w_n^3} \frac{\rho}{2\pi^2} \frac{1}{r_0} \tag{11}$$

In equations 10, 11 and subsequent equations, the lower index n indicates the quantities of the n -th crack. Let p_0 be the wellbore fluid pressure at a representative depth, p_{0n} be the fluid pressure at the depth of the n -th crack and Δd_n be the relative depth of the n -th crack measured from the representative depth. From eq.(9), we have

$$p_0 = S_n + f_n Q_n^2 - \rho g \Delta d_n \tag{12}$$

where g is the acceleration due to gravity. Furthermore, the injection flow rate Q_{in} is equal to the sum of the flow rates of fluid flowing into the cracks. Thus, we have

$$\sum_{n=1}^{N} Q_n = Q_{in} \tag{13}$$

According to Willis-Richards et al. (1996), a plane of weakness along which the following condition is satisfied does not slip and is stable:

$$\tau < (\sigma - p)\tan(\phi + i) \tag{14}$$

This can be rewritten as follows:

$$p_0 - f Q_n^2 < S_n - \rho g \Delta d_n \tag{15}$$

It is readily understood that each plane of weakness starts to slip when the representative wellbore pressure p_0 reaches to $S_n - \rho g \Delta d_n$. In other words, among the planes of weakness, slip takes place first along the one with smallest $S_n - \rho g \Delta d_n$ and, after that, slip takes place sequentially in the order of $S_n - \rho g \Delta d_n$ with increasing representative wellbore pressure p_0 . The relationships Q_n vs. Q_{in} and p_0 vs. Q_{in} are determined by solving eqs. (12) and (13).

Now let us apply the model to a fictitious data set to demonstrate the basic nature of the model. Suppose that there are three planes of weakness having different orientations with respect to the principal axes of stress. Here, the differences in the orientation is expressed by the difference in S_n , i.e., S_1 =20MPa, S_2 =21MPa and S_3 =22MPa. The depth difference, Δd_n , is set to be zero for simplicity, and the aperture w and rougness ratio, k/D_h are set to be 2mm and 0.5, respectively. The results are summarized in Figure 2, where Q_1 , Q_2 and Q_3 are the flow rates of fluid flowing into the first, second and third cracks,
respectively. When the injection flow rate Q_{in} is less than 15 m^3/h , only one crack is active to accept the injected fluid.

But when the injection flow rate is larger than 35 m^3/h , all of the three cracks accept the injected fluid. For the

intermediate flow rate of 15 – 35 m^3/h , two cracks accept the injected fluid. It is also shown that the flow rate flowing into each of the three cracks becomes almost equal to each other with increasing injection flow rate.

3. ANALYSIS OF THE RESERVOIR IN YUNOMORI FIELD

Let us apply the model constructed in the previous section to the reservoir in Yunomori field which is the location of the HWR project of NEDO. The reservoir was created by hydraulic stimulation at well TG-2, where the largest injection flow rate was 240 m^3/h (Shinohara and Takasugi, 1993). After the hydraulic stimulation, spinner logging was conducted at a flow rate of 90 m^3/h (Figure 3). The logs show

that the injected fluid flows into the formation through the four zones at depths of 1060m, 1135m, 1160m and 1170m. Figure 4 shows the variations of wellbore pressure and flow rate with respect to the depth obtained from the logs. It can be seen that fluid flows into the formation at a flow rate of $32.2\,m^3/h$ under a wellbore pressure of 22.7MPa at the shallowest zone of 1060m. The flow rates are $32.2\,m^3/h$ at 23.5MPa, $13.7\,m^3/h$ at 23.8MPa and $11.9\,m^3/h$ at 23.9MPa at depths of 1135m, 1160m and 1170m, respectively. All the cracks of the four zones were identified by FMI (Formation Micro Imager) survey (Okabe et al., 1993). Figure 5 shows the poles of the cracks in the lower hemisphere of the Shumidt net. Roughly speaking, there are two groups of cracks, i.e., transverse which are cracks that are almost horizontal and vertical and those which are almost vertical and are striking NW-SE. The stresses have been measured by the ASR (Anelastic Strain Recovery) method by using oriented core samples from depths of 850m and 1218m (Matsuki, 1993). The stress state in the four zones were estimated on the assumption that stress ratio among the principal stresses and stress orientation are independent of depth. The resulting stress state is summarized in Figure 6. In order to apply the model, we need to know the aperture of the cracks, as well as the effective angle of friction ϕ_{eff} that is defined as the sum of the angle of friction and the shear dilation angle (Goodman, 1980). Because we do not have a direct information for both of them, we have to estimate them indirectly. The effective angle of friction can be set to be 55° (Willis-Richards et al., 1996, Murphy, 1982 and Goodman, 1980). The aperture of the cracks is determined from the spinner log data under the assumption that all cracks in each zone have the same aperture. The results, using the following values, are summarized in Table 1: $k/D_h = 0.5$ and $\rho = 1.0g/cm^3$ and $r_0 = 0.1m$. As mentioned in the previous section, slip takes place according to the equation $S_n - \rho g \Delta d_n$. Figure 7 shows the relationship between the dip angle θ of cracks and the order of slip n. In general, the cracks with larger dip angle slip first followed by the cracks with smaller dip angle.

As stated in the previous section, the variations of the wellbore pressure and flow through each crack with respect to the injection flow rate Q_{in} are determined by using eqs. (12) and (13) under constant injection flow rate. The result is shown in Figure 8, where Q_d denotes the flow rate of fluid flowing into each of the four zones. When the total injection flow rate Q_{in} is as small as $100\,m^3/h$, most of the injected fluid flows into the two shallower zones. But when the total injection flow rate is as large as $500\,m^3/h$, the situation changes drastically, i.e., about 70% of the injected fluid flows into the two deeper zones. The transition takes place at around $Q_{in} = 200-300 m^3/h$. Figure 9 shows the dip of the activated cracks in the four zones at the injection flow rates of 90, 240 and $500\,m^3/h$. The wellbore pressure at depth of 1060 m is chosen to be the representative pressure, p_0. The numbers shown in the figure are the percentage of the flow accepted in each zone. A clear image of the transitional morphology of the reservoir can be seen in Figure 9, especially in the two deeper zones. As the injection flow rate is increased, the transverse cracks in the two deeper zones become part of the reservoir that accepts the fluid.

Figure 10 (Niitsuma, 1993) shows the 3-D source location of AE (Acoustic Emission) events observed during the hydraulic stimulation conducted at an injection flow rate of $240\,m^3/h$. According to this figure, the reservoir consists of three almost vertical subsets of cracks and a subset of transverse cracks. The morphology of the reservoir for the injection flow rate of $240\,m^3/h$ shown in Figure 9 agrees fairly well with the 3-D source location of AE events.

Let us discuss the difference between the result estimated by the pure opening mode model employed in the paper by Hayashi and Taniguchi (1999) and that obtained by shear mode model in this paper. By comparison, it is seen that the transverse cracks in the shallowest zone become active at much smaller injection flow rate in the shear mode model than in the pure opening mode model. Furthermore, the contribution of the deeper two zones as estimated by the shear mode model is far larger than that estimated by the pure opening mode model. For example, 70% of the injected fluid flows into the two deeper zones in the shear mode model at an injection rate of $500\,m^3/h$. However, it is only 52% according to the pure opening mode model.

4. CONCLUSION

Based on the concept that the increase in the aperture of geothermal reservoir cracks is primarily due to slip induced along pre-existing planes of weakness, we constructed a simple model that could describe the transitional morphology of a geothermal reservoir due to hydraulic stimulation. We applied the model to examine and to understand what happened during hydraulic stimulation at well TG-2 in the Yunomori test site of the HWR project by NEDO. The main conclusions are summarized as follows:

(1) At well TG-2, the two shallower zones among the four zones which were identified to accept the injected fluid play a main role for a small injection flow rate. But for a large injection flow rate the two deeper zones assume a bigger role. This transition takes place at around the injection flow rate of $200\text{-}300\,m^3/h$.
(2) The main feature of the morphology of the reservoir deduced from the present analysis agrees fairly well with the estimate based on the source location of AE (Acoustic Emission) events which were observed during hydraulic stimulation.

ACKNOWLEDGEMENT

The authors wish to thank Professor H. Niitsuma for providing Figure 10. They also wish to thank Mr. K. Kuroki for his help in preparing the manuscript.

REFERENCES

Duchane, D. (1991). International Programs in Hot Dry Rock Technology Development, *Geother. Resouor. Coun. Bull.*, Vol. 20, pp.135-142.

Fehler, M., House, L., and Kaieda, H. (1987). Determining Planes along Which Earthquakes Occur: Method and Application to Earthquakes Accompanying Hydraulic Fracturing, *J. Geophys. Res.*, Vol. 92, pp. 9407-9414.

Goodman, R. E. (1980). *Introduction to Rock Mechanics*, John Wiley and Sons, New York.

Hayashi, K. and Taniguchi, A. (1999). Response of a Geothermal Reservoir Consisting of Multiple Cracks to Hydraulic Stimulation, *Geother. Sci. & Tech.*,Vol. 6, pp.163-179.

Jung, R. (1986). Erzeugung eines Grobflachigen Kunstlichen Risses im Falkenberger Granite durch Hydraulisches Spalten und Untersuchung seiner Mechanischen und Hydraulischen Eigenschaften, Diss. Ruhr-Univ. Bochum.

Matsuki, K. and Takeuchi, K. (1993). Three-dimensional In Situ Stress Determination by Anelastic Strain Recovery of a Rock Core, *Int. J. Rock Mech. Min. Sci. & Geomech. Abstr.*, Vol. 30, pp.1019-1022.

Miyairi, M. (1993). Reservoir Characterization by Downhole Measurements in Hijiori HDR Test Site, presented at *2nd Hot Dry Rock Geothermal Energy Forum*, Yamagata, Japan.

Niitsuma, H. (1993). private communication.

Okabe, T., Shinohara, N. and Takasugi, S. (1993). Measurement Results and Evaluation of BHTV Logging and FMI Logging at TG-2 Well, *Proc. of 88th Symp. of Soc. Explor. Geophys. Japan*, pp. 361-366 (in Japanese with English abstract).

Murphy, H. (1982). Modelling Hydraulic Fructuring in Jointed Rock, Preliminary FRIP Results, *Internal Report in CSM*, 34 pp.

Shinohara, S. and Takasugi, S. (1993). Fracture Design and the Results of Mini Hydraulic Fracturing Employed for the TIGER Project, *Proc. of 88th Symp. of Soc. Explor. Geophys*. Japan, pp.343-348 (in Japanese with English abstract).

Takahashi, H. and Hashida, T. (1992). New Project for Hot Dry Rock Geothermal Reservoir Design Concept, *Proc. 17th Stanford Workshop on Geothermal Reservoir Engineering*, Stanford, pp. 39-44.

Willis-Richards, J. and Wallroth, T. (1995). Approaches to the Modelling of HDR Reservoirs : a Review, *Geothermics*, Vol. 24, pp. 307-332.

Willis-Richrds, J. Watanabe, K. and Takahashi, H. (1996). Progress toward a Stchastic Rock Mechanics Model of Engineered Geothermal Systems, *J. Geophy. Res.*, Vol. 101, pp. 17481-17496.

Table 1. Aperture of cracks at each zone estimated from spinner logs. The spinner logging was conducted at the injection flow rate of 90 m^3/h .

Depth (m)	1060	1135	1160	1170
Aperture (mm)	0.17	0.55	1.75	2.16

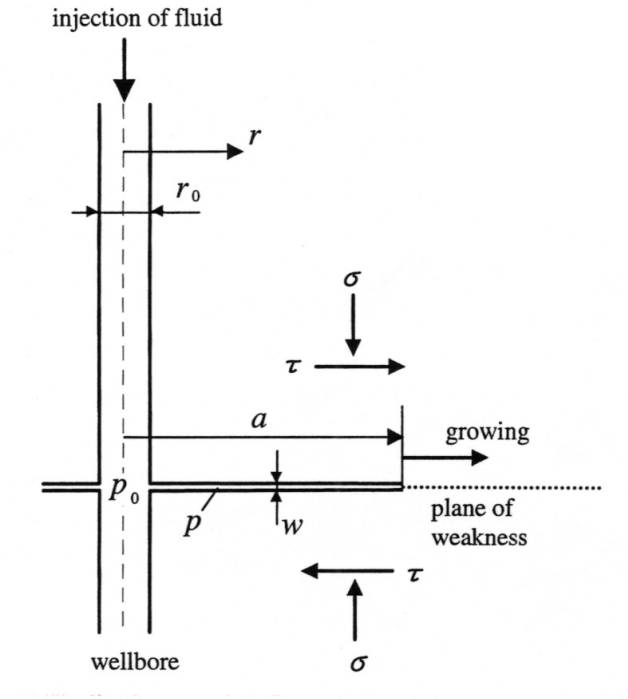

Figure 1. A crack growing up in shear mode along a plane of weakness.

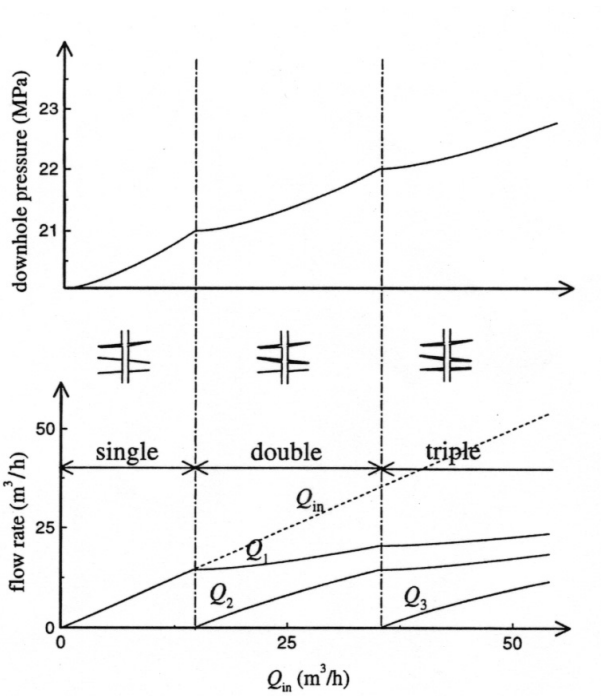

Figure 2. Demonstration of transitional morphology of a reservoir consisting of multiple cracks, where S_1 , S_2 and S_3 are set to be 20, 21 and 22MPa, respectively. The aperture w and k/D_h are set to be 2mm and 0.5, respectively.

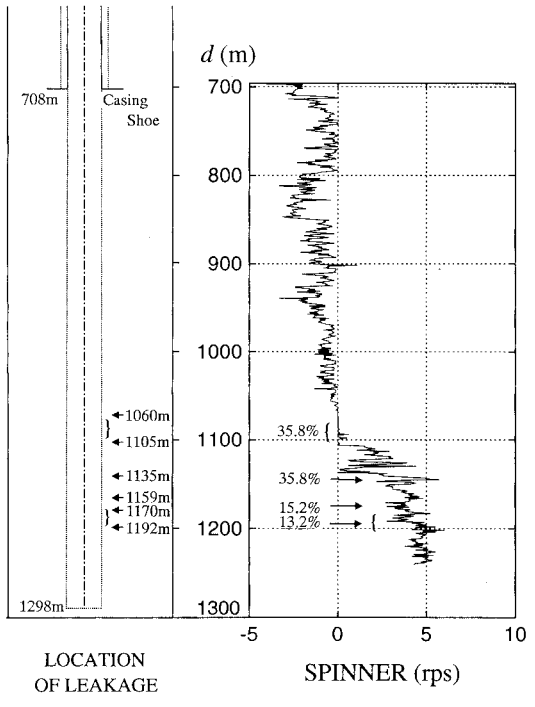

Figure 3. Summary of the results of the spinner logging. The injection flow rate was 90 m³/h (Shinohara and Takasugi, 1993). The four zones (1060-1105, 1135, 1159 and 1170-1192m) are accepting fluid. In the main text, these four zones are denoted as the zones of 1060, 1135, 1160 and 1170m, respectively.

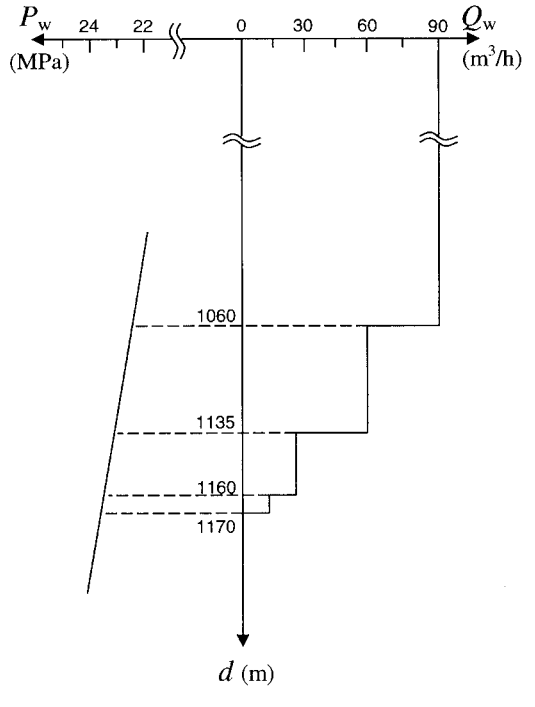

Figure 4. Variations of flow rate Q_w and fluid pressure p_w in well TG-2 during the spinner logging, with respect to depth d.

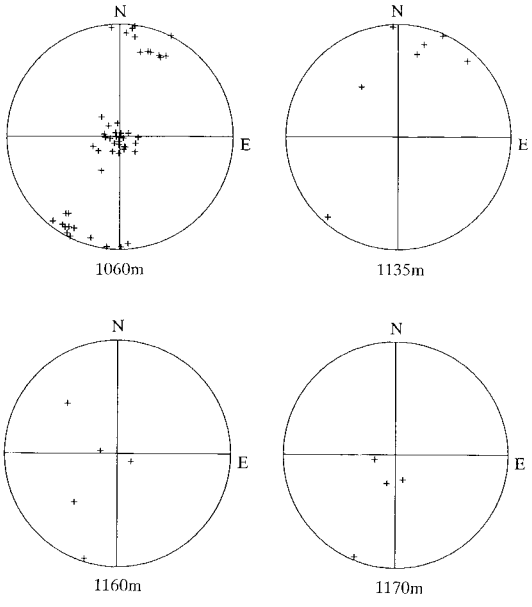

Figure 5. Polar plots of cracks observed at the four zones by FMI survey (Shumidt net, lower hemisphere) (Okabe et al., 1993). Roughly speaking, there are two sets of cracks, i.e., nearly horizontal ones and nearly vertical ones striking in NW-SE.

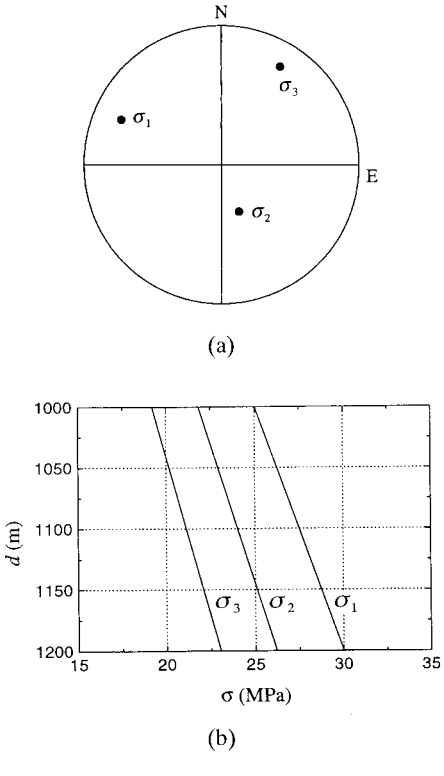

Figure 6. Stress state around well TG-2 in the depth range covering the four zones. The lower figure shows the variation of the principal stress magnitude with depth. The upper figure shows the orientation of the principal axes of stress (Shumidt net, lower hemisphere).

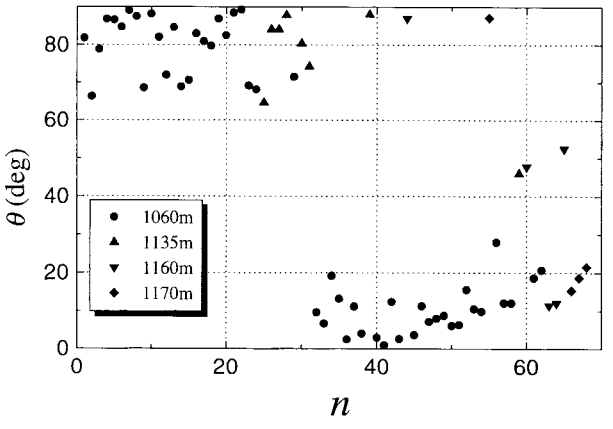

Figure 7. Relationship between the dip angle θ and the order of slip n. As a whole, the cracks with larger dip angle slip first and then the cracks with smaller dip angle start to slip.

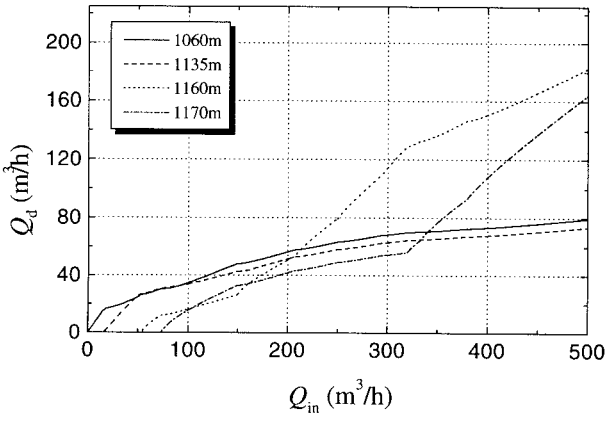

Figure 8. Variations of the fluid flow rate Q_d accepted in each zone with respect to the injection flow rate Q_{in}.

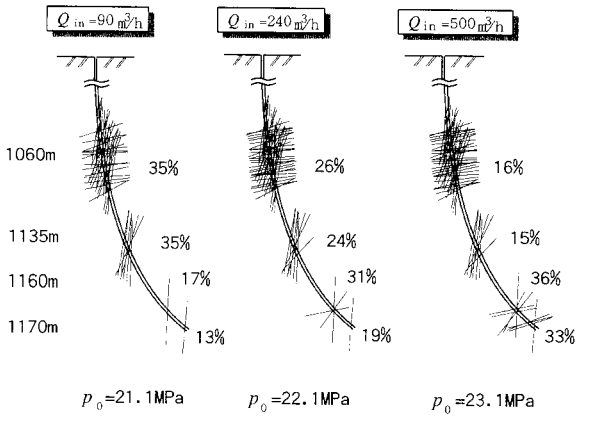

Figure 9. Schematic presentation of the variation of the reservoir morphology at the Yunomori field.

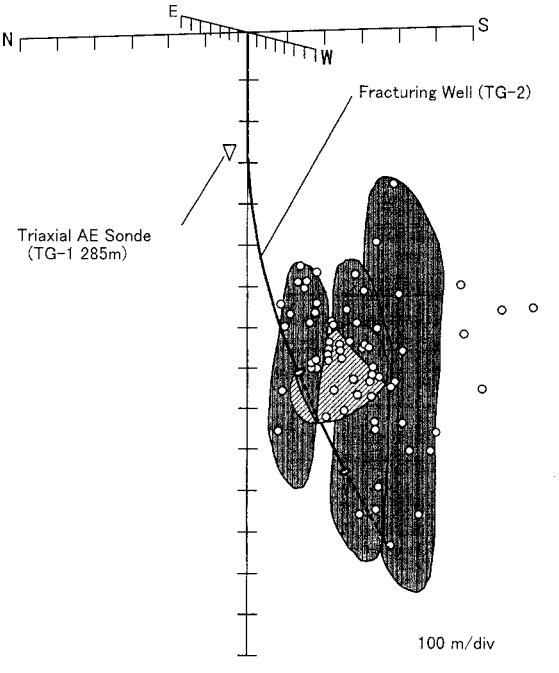

Figure 10. Reservoir morphology estimated from AE events observed during hydraulic stimulation (Niitusma, 1993). The small circles are the hypercenters of the AE events.TG-1 is the observation well in which a triaxial AE sonde was set at the depth of 285m.